

# Combined Measurement of Neutral and Charged Current Cross Sections at HERA

Jolanta Sztuk-Dambietz<sup>1</sup>

*Hamburg University, Institute of Exp. Physics, Luruper Chaussee 149, 22761 Hamburg, Germany*

**Abstract.** A combination of the inclusive cross sections measured by the H1 and ZEUS Collaborations in neutral and charged current deep-inelastic  $e^\pm p$  scattering at HERA is presented. The combination uses data from unpolarised  $e^\pm p$  scattering taken during the HERA-I phase as well as measurements with longitudinally polarised electron or positron beams from the HERA-II running period. The data span six orders of magnitude in negative four-momentum-transfer squared,  $Q^2$ , and in Bjorken  $x$ . The combination method takes the correlations of systematic uncertainties into account, resulting in an improved accuracy. The inclusion of the large HERA-II data set leads to an improved uncertainty especially at large  $Q^2$ . The combined data are the sole input to a NLO QCD analysis which determines a new set of parton distribution functions, HERAPDF1.5.

**Keywords:** Deep Inelastic  $e^\pm p$  Scattering, Neutral Current, Charged Current, Proton Structure Functions, HERA

**PACS:** 13.60.Hb

## 1. INTRODUCTION

Deep inelastic scattering (DIS) at HERA has been central to the exploration of proton structure and the dynamics of quark-gluon interaction as described in perturbative Quantum Chromodynamics (QCD). At HERA, inelastic  $ep$  interactions are studied at a centre-of-mass energy,  $\sqrt{s} \approx 320 \text{ GeV}$ , where  $s = 4E_e E_p$  with the lepton beam energy  $E_e \approx 27.5 \text{ GeV}$  and the proton beam energy  $E_p = 920 \text{ GeV}$  for most of the running. The operation of HERA proceeded in two phases, HERA I, from 1992-2000, and HERA II, from 2002-2007. In general, analyses at low and intermediate  $Q^2$ ,  $Q^2 \leq 150 \text{ GeV}^2$ , could be performed using relatively small data sets. Therefore, high precision analyses were done using already HERA-I data only. The analyses at higher  $Q^2$ ,  $Q^2 \geq 150 \text{ GeV}^2$ , were in general more constrained by the statistics available. The usage of HERA-II data, nearly  $350 \text{ pb}^{-1}$  per experiment, improved the precision significantly in this regime. HERA-II also provided lepton beam polarisation; typically the polarisation reached 30-40%. The total (HERA-I +II) luminosity collected by the two experiments, H1 and ZEUS, was approximately  $500 \text{ pb}^{-1}$ , each.

## 2. DIS CROSS SECTIONS AND STRUCTURE FUNCTIONS

The kinematics of lepton hadron scattering is described in terms of the variables  $Q^2$ , the four-momentum transfer squared of the exchanged vector boson, Bjorken  $x$ , the frac-

---

<sup>1</sup> on behalf of the H1 and ZEUS Collaborations

tion of the momentum of the incoming nucleon taken by the struck quark (in the Quark Parton model (QMP)), and the inelasticity  $y$  which measures the energy transfer between the lepton and hadron systems.

The neutral current deep inelastic  $e^\pm p$  scattering cross section, at tree level, is given by a linear combination of generalised structure functions. For unpolarised beams it can be expressed as

$$\frac{d^2\sigma_{\text{NC}}^{e^\pm p}}{dx dQ^2} = \frac{2\pi\alpha^2}{xQ^4} (Y_+ \tilde{F}_2 \mp Y_- x\tilde{F}_3 - y^2 \tilde{F}_L), \quad (1)$$

where  $\alpha$  is the electromagnetic coupling constant, and  $Y_\pm = 1 \pm (1-y)^2$ . The structure functions  $\tilde{F}_2$  and  $x\tilde{F}_3$  are directly related to quark distributions, and their  $Q^2$  dependence, or scaling violation, is predicted by perturbative QCD. For low  $x$ ,  $x \leq 10^{-2}$ ,  $F_2$  is sea quark dominated, but its  $Q^2$  evolution is controlled by the gluon contribution, such that HERA data provide crucial information on low- $x$  sea-quark and gluon distributions. At high  $Q^2$ , the structure function  $x\tilde{F}_3$  becomes increasingly important, and gives information on the sum of the valence quark distributions,  $u_v = u - \bar{u}$  and  $d_v = d - \bar{d}$ . The  $F_L$  contribution is significant only at high  $y$  and can be neglected at high  $Q^2$  and high  $x$ .

The Charged Current (CC) interactions provide a separation of the flavours of the valence distributions at high  $x$ , since their (LO) cross sections are given by

$$\frac{d^2\sigma_{\text{CC}}^{e^+ p}}{dx dQ^2} = \frac{G_F^2}{2\pi} \left[ \frac{M_W^2}{M_W^2 + Q^2} \right]^2 [(\bar{u} + \bar{c}) + (1-y)^2(d + s)], \quad (2)$$

$$\frac{d^2\sigma_{\text{CC}}^{e^- p}}{dx dQ^2} = \frac{G_F^2}{2\pi} \left[ \frac{M_W^2}{M_W^2 + Q^2} \right]^2 [(u + c) + (1-y)^2(\bar{d} + \bar{s})], \quad (3)$$

where  $G_F$  is the Fermi coupling constant,  $M_W$  is the mass of the  $W^\pm$  boson and the terms with the quark distributions describe the composition of quarks in the proton probed by the  $W^+$  or  $W^-$  boson. The combined NC and CC measurements provide the sea quark distribution functions,  $x\bar{U} = x(\bar{u} + \bar{c})$  and  $x\bar{D} = x(\bar{d} + \bar{s})$ , and the valence quark distributions,  $xu_v$  and  $xd_v$ . A QCD analysis in the DGLAP formalism also allows the gluon momentum distribution,  $xg$ , in the proton to be determined from scaling violations.

### 3. COMBINATION OF H1 AND ZEUS CROSS SECTIONS

Prior to the combination, the H1 and ZEUS HERA-I [1] and HERA-II high- $Q^2$  [2, 3, 4, 5, 6] DIS data were transformed to a common grid of  $(x, Q^2)$  points and corrected to a common centre-of-mass energy corresponding to  $E_p = 920$  GeV and then averaged<sup>2</sup>.

For the combination of the data sets, the  $\chi^2$  minimisation method described in [1] was used. The  $\chi^2$  function takes into account the correlated systematic uncertainties of

---

<sup>2</sup> The NC data for  $y \geq 0.35$  are kept separate for the part of the data where the proton beam energy was  $E_p = 820$  GeV (until 1997).

the H1 and ZEUS cross-section measurements. For a single data set, the  $\chi^2$  is defined as

$$\chi_{\text{exp}}^2(\mathbf{m}, \mathbf{b}) = \sum_i \frac{\left[ m^i - \sum_j \gamma_j^i m^i b_j - \mu^i \right]^2}{\delta_{i,\text{stat}}^2 \mu^i (m^i - \sum_j \gamma_j^i m^i b_j) + (\delta_{i,\text{uncor}} m^i)^2} + \sum_j b_j^2. \quad (4)$$

Here  $\mu^i$  is the measured value at a point  $i$  and  $\gamma_j^i$ ,  $\delta_{i,\text{stat}}$  and  $\delta_{i,\text{uncor}}$  are relative correlated systematic, relative statistical and relative uncorrelated systematic uncertainties, respectively. The function  $\chi_{\text{exp}}^2$  depends on the predictions  $m^i$  for the measurements (denoted as the vector  $\mathbf{m}$ ) and the shifts  $b_j$  (denoted as the vector  $\mathbf{b}$ ) of the correlated systematic error sources. For the reduced cross-section measurements  $\mu^i = \sigma_r^i$ ,  $i$  denotes a  $(x, Q^2)$  point, and the summation over  $j$  extends over all correlated systematic sources. The predictions  $m^i$  are given by the assumption that there is a single true value of the cross section corresponding to each data point  $i$  and each process, neutral or charged current  $e^+p$  or  $e^-p$  scattering.

The minimisation also provides a model-independent check of the data consistency. The input data from H1 and ZEUS are consistent with each other at  $\chi^2/n_{\text{dof}} = 967.5/1032$ . Since H1 and ZEUS have employed different experimental techniques, using different detectors and methods of kinematic reconstruction, the combination leads to a significantly reduced uncertainty.

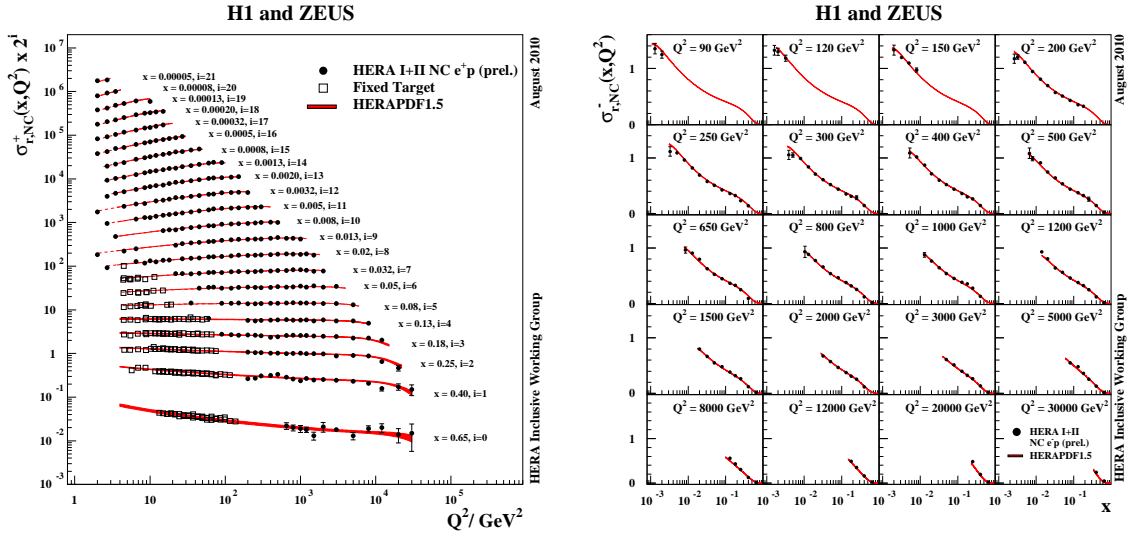


**FIGURE 1.** HERA combined NC  $e^+p$  reduced cross section and fixed-target [7, 8] data as a function of  $Q^2$  (left plot) and NC  $e^-p$  reduced cross sections as a function of  $x$  in bins of  $Q^2$  (right plot). The HERAPDF1.5 [9] fit is superimposed. The bands represent the total uncertainty of the fit. Dashed lines are shown for  $Q^2$  values not included in the QCD analysis.

The kinematic range of the NC data is  $6 \cdot 10^{-7} \leq x \leq 0.65$  and  $0.045 \leq Q^2 \leq 30000 \text{ GeV}^2$ , for values of  $y$  between 0.005 and 0.95. HERA combined NC  $e^\pm p$  reduced cross sections as a function of  $Q^2$  and  $x$  are shown in Figure 1. The kinematic range of the CC data is  $1.3 \cdot 10^{-2} \leq x \leq 0.65$  and  $300 \leq Q^2 \leq 30000 \text{ GeV}^2$ . HERA combined

CC  $e^\pm p$  reduced cross sections as a function of Bjorken  $x$  in bins of  $Q^2$  are shown in Figure 2.

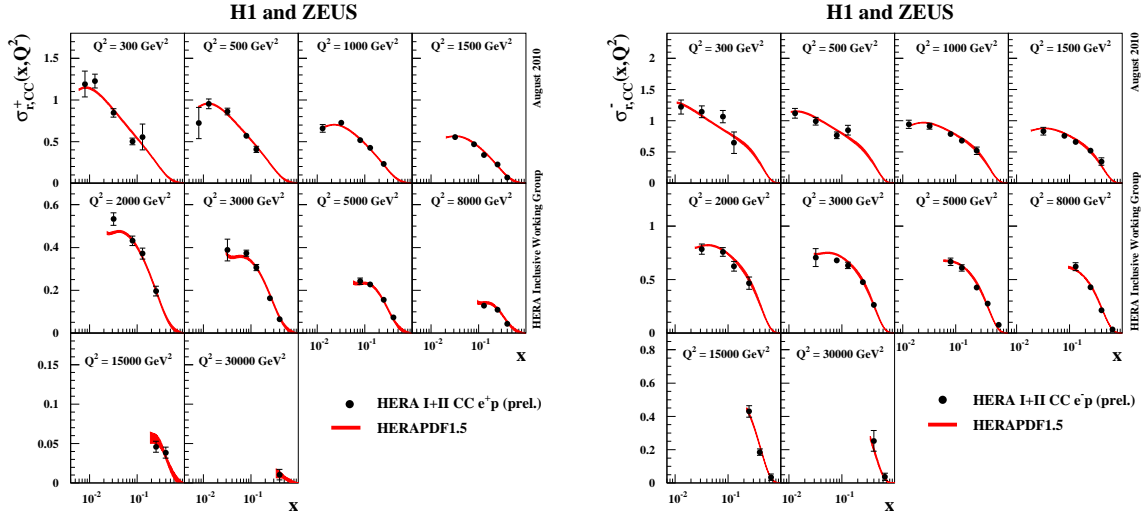


**FIGURE 2.** HERA combined CC  $e^- p$  (left plot) and  $e^+ p$  (right plot) reduced cross sections as a function of  $x$  in bins of  $Q^2$ . The HERAPDF1.5 fit is superimposed. The bands represent the total uncertainty of the fit.

## 4. SUMMARY

Inclusive cross sections of neutral and charged current  $e^\pm p$  scattering measured by the H1 and ZEUS Collaborations were combined. The combination comprises most of the inclusive data from HERA. The input data from H1 and ZEUS span six orders of magnitude in  $Q^2$ , and in Bjorken  $x$  and are consistent with each other at  $\chi^2/n_{\text{dof}} = 967.5/1032$ . The total uncertainty of the combined data set reaches 1% for NC scattering in the region best measured,  $20 < Q^2 < 100 \text{ GeV}^2$ . The inclusion of the large HERA-II data set leads to an improved uncertainty especially at large  $Q^2$ . The combined data were the sole input to a NLO QCD analysis which provided a new set of parton distributions HERAPDF1.5 [9].

## REFERENCES

1. F. D. Aaron, et al., *JHEP* **01**, 109 (2010), 0911.0884.
2. S. Chekanov, et al., *Eur. Phys. J.* **C62**, 625–658 (2009), 0901.2385.
3. S. Chekanov, et al., *Eur. Phys. J.* **C61**, 223–235 (2009), 0812.4620.
4. H. Abramowicz, et al., *Eur. Phys. J.* **C70**, 945–963 (2010), 1008.3493.
5. *H1-prelim-09-042* (2009).
6. *H1-prelim-09-043* (2009).
7. A. Benvenuti, et al., *Phys. Lett.* **B223**, 485 (1989).
8. M. Arneodo, et al., *Nucl. Phys.* **B483**, 3 (1997).
9. *H1-prelim-10-142*, *ZEUS-prel-10-018* (2010).